euspen's 26th International Conference & Exhibition, Krakow, PL, June 2026
www.euspen.eu

Modeling and Quantification of Parameter-Induced Thermal Errors in a Hydrostatic Turntable System

Jun Zha[1,2], Changhui Ke[3], Lipu Song[1,2], Chengwei Kang[1,2]

[1]*School of Mechanical Engineering, Xi'an Jiaotong University, Xi'an 710049, China*
[2]*Xi'an Jiaotong University-Genertec Joint Research Institute, Xi'an 710049, China*
[3]*School of Mechanical and Precision Instrument Engineering, Xi'an University of Technology, Xi'an 710048, China*

jun_zha@xjtu.edu.cn, chengwei.kang@xjtu.edu.cn

Abstract

Thermal errors in hydrostatic turntable systems are a primary impediment to achieving sub-micron accuracy in ultra-precision machine tools, directly impacting workpiece dimensional stability. These errors are predominantly caused by heat generated from the oil pump and viscous friction within the bearing's oil film during operation. This research aims to systematically model and quantify the influence of key operating parameters, specifically oil supply pressure and oil film gap, on the system's thermo-mechanical behavior.
The methodology is centered on a thermo-mechanical coupling model developed to simulate the system's response. The process began by establishing a detailed temperature field model through a thermal balance calculation, which quantified the heat generated by system components against heat dissipated. This thermal analysis was then coupled with a structural model, using the calculated temperature distribution as a thermal load to accurately predict the resulting deformation and strain. A parametric study was performed using this model to analyze the turntable's behavior under a range of different service conditions.
The results effectively map the internal temperature and total deformation fields during turntable operation, establishing a direct monotonic correlation between rotation speed, oil supply pressure, oil film gap, and the resulting thermal error. Analysis of the internal temperature confirmed a pronounced thermal stratification: the highest temperature occurs at the oil sealing surface, followed by the mandrel, and the frame. The temperature exhibits a clear gradient distribution, decreasing from the axis end outward. Total deformation is maximized at the motor, minimized at the base, and generally increases toward the mandrel end. The study identified that while elevated rotation speed leads to a greater temperature rise, a larger oil film gap is beneficial for decelerating this rise. Significantly, oil supply pressure was determined to be the more dominant factor governing both temperature increase and thermal deformation compared to the oil film gap and the rotation speed. This work provides a quantitative framework for optimizing operational parameters to minimize thermal errors, thereby contributing valuable theoretical insights for the design and control of high-precision hydrostatic turntable systems.

Hydrostatic Turntable; Thermal Error; Thermo-mechanical Coupling Model; Parametric Analysis

1. Introduction

Thermal error represents the primary obstacle preventing hydrostatic rotary table systems from achieving sub-micron accuracy in ultra-precision machine tools, directly impacting workpiece dimensional stability[1]. The thermal error of hydrostatic rotary table refers to that the heat energy generated by bearing friction and oil pump operation during the working process of the rotary table will increase the temperature of lubricating oil, spindle and bearing seat in the bearing clearance through heat transfer, resulting in thermal error issues such as intensified thermal deformation and reduced viscosity of lubricating medium, which seriously affects the machining accuracy of machine tools[2][3]. Research indicates that thermal error accounts for 40% to 70% of the total error in precision machining, representing the single largest and most challenging error source to suppress [4]. Consequently, analyzing and investigating the thermal error of hydrostatic turntables is of considerable significance for developing effective thermal error suppression methods and enhancing the machining accuracy of machine tools. Thermal error analysis of hydrostatic rotary table operation continues to be a central research hotspot[5], with existing work, such as the mathematical model for fan-shaped oil pads by Bao et al, providing foundational insights[6].

Despite these efforts, current research predominantly relies on mathematical modeling and simulation to explore the effects of single parameters (e.g., oil film pressure or clearance). Comprehensive, comparative studies that analyze the combined influence of multiple operational parameters across various working conditions are still insufficient. This study aims to bridge this gap by systematically modeling and quantifying the integrated impact of essential operating variables, specifically oil supply pressure, oil film clearance, and rotation speed, on the system's thermal error. We achieve this by establishing a refined thermal error model for the hydrostatic turntable, investigating the internal thermal error distribution, and quantifying the influence of different working condition parameters on the turntable's thermal performance.

2. Thermal error analysis of the hydrostatic turntable

2.1. Hydrostatic turntable structure

The hydrostatic turntable system examined in this paper is illustrated in Figure 1, and primarily comprises the table, the hydrostatic bearing, and the frame. The hydrostatic bearing itself is composed of an inner radial bearing and a thrust bearing, which are symmetrically distributed along the axial direction. In operation, an external oil supply system pressurizes the bearing recess to establish a lubricating oil film. This film allows the mandrel to float and maintain a small, controlled gap, thereby achieving a state of complete liquid friction. Subsequently, the built-in motor housed within the frame drives the bearing and the workbench to rotate axially.

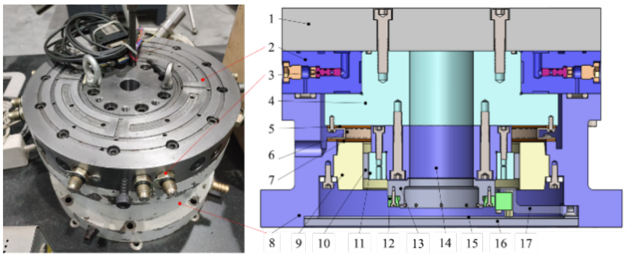

1-Tabletop; 2-Hydrostatic bearing; 3-Annular slit restrictors; 4-Bearing rotor; 5-Upper seal ring; 6-Oil blocking plate; 7-Lower seal ring; 8-Base; 9-Motor stator; 10-Motor armature; 11-Motor rotor; 12-Reading head; 13-Fixed shaft; 14-Mandrel; 15-Rubber pad; 16-Bottom plate; 17-Reading headstock

Figure 1. Hydrostatic turntable structure diagram

2.2. Thermal error model of hydrostatic turntable

Under the service conditions of the hydrostatic turntable, the temperature rise primarily arises from bearing friction and other external environmental heat sources. Among these, because the heat generated by external environmental sources and other secondary sources is much smaller than the heat generated by the bearing, it can be reasonably neglected. This simplifies the mixed temperature field model, which is typically affected by multiple variables and complex fields, into a single temperature field model dominated by bearing friction. The temperature field of the turntable is then modeled by calculating the heat generation of the radial bearing and the thrust bearing.

When lubricating oil flows inside the hydrostatic bearing, it may exhibit laminar flow, turbulent flow, or a transitional state between the two. The flow field characteristics vary with the flow state, and accordingly, different calculation methods are required. Therefore, to establish a temperature field model, it is necessary to first determine the fluid flow state using the Reynolds number formula shown in Eq. (1). If the calculated Reynolds number is less than 2000, the fluid is considered to be in laminar flow. If it exceeds 4000, the fluid is considered turbulent. When the Reynolds number lies between 2000 and 4000, the fluid is assumed to be in the transitional regime. In this study, the flow velocity is assumed to be 20 m/s, yielding a Reynolds number of 12.5, which is far below 2000. Therefore, the fluid inside the bearing is considered to be in laminar flow, and static performance calculations are applicable.

$$\mathrm{Re}=\rho v_l l/\mu \tag{1}$$

Where ρ is the density of the hydraulic oil, v_l is the fluid velocity, l is the equivalent radius through the interface, and μ is the dynamic viscosity of the hydraulic oil.

After determining the flow state of the lubricating oil inside the bearing, to establish the temperature field model of the bearing, the following isothermal assumptions need to be made :

Both the pump power and friction power are converted into thermal energy, while other less influential heat sources are neglected. It is assumed that all resulting heat is absorbed entirely by the lubricating oil within the hydrostatic bearing system.

Thermodynamic properties, such as the convective heat transfer coefficients of the lubricating medium and the surrounding air, are assumed to remain constant and independent of temperature. The temperature rise of the hydraulic oil due to internal friction power adheres to the law of conservation of energy.

The temperature rise of the bearing is primarily attributed to the liquid friction power N_f and the oil pump power N_p. N_f represents the power loss due to liquid friction during the relative sliding motion of the mandrel and is dependent on the rotational speed. N_p represents the power consumption caused by the laminar flow of the lubricating oil film driven by the oil supply system. Since the radial velocity of the bearing bush and the linear velocity of the thrust recess vary with position, N_f must be calculated separately for each component. N_p denotes the power consumption of the oil supply system. The detailed calculation is presented in Eq. (2) and Eq. (3).

$$\begin{cases} N_{fj} = n \cdot \mu \cdot v^2 \left(\dfrac{A_1}{h_0} + \dfrac{A_2}{h_0 + z_1} \right) \\ N_p = p_s \cdot n \cdot q \\ \Delta T = \dfrac{N_f + N_p}{c \rho q} \end{cases} \tag{2}$$

$$\begin{cases} N_{fz} = n \sum\limits_{i=1}^{5} P_{zi} \\ P_{z1} = P_{z2} = \int_{R_1}^{R_4} \mu \left(\dfrac{2\pi n R}{60} \right)^2 \dfrac{R\alpha_1}{h_0} dR \\ P_{z3} = \int_{R_3}^{R_4} \mu \left(\dfrac{2\pi n R}{60} \right)^2 \dfrac{R\alpha_2}{h_0} dR \\ P_{z4} = \int_{R_2}^{R_3} \mu \left(\dfrac{2\pi n R}{60} \right)^2 \dfrac{R\alpha_2}{h_0 + z_1} dR \\ P_{z5} = \int_{R_1}^{R_2} \mu \left(\dfrac{2\pi n R}{60} \right)^2 \dfrac{R\alpha_2}{h_0} dR \end{cases} \tag{3}$$

Where N_{fj} is the liquid friction power of the radial bearing, n is the number of oil recesses, v is the rotational speed, A_1 and A_2 represent the areas of the hydraulic support surface and the recess of a single recess, respectively. h_0 is the oil film thickness, z_1 is the recess depth, p_s is the oil supply pressure, q is the flow rate of a single oil recess, ΔT is the temperature rise of the bearing bush, and c is the specific heat capacity of the lubricating oil at constant pressure, N_{fz} is the thrust bearing liquid friction power, P_{zi} is the liquid friction power of each region of thrust bearing recess.

Once the temperature rise of the bearing is obtained, the corresponding thermal deformation can be calculated based on the theory of thermal expansion using Eq. (4):

$$\Delta L = \alpha L_0 \Delta T \tag{4}$$

where ΔL is the linear thermal deformation of the object, α is the coefficient of thermal expansion, and L_0 is the initial length.

3. Thermal error finite element analysis of the hydrostatic turntable

To investigate the temperature and deformation distributions of the hydrostatic turntable under various operating conditions, a steady-state thermal-structural coupling simulation was performed using ANSYS. The meshed model is presented in Figure 2. Different components of the turntable were meshed using separate techniques, specifically sweeping, multi-region, and automatic methods, to ensure mesh quality. Furthermore, four layers of surface meshing were applied to individual thin-walled parts. The global element size was set to 5 mm, with key regions such as the bearing oil sealing surfaces and the oil cavities refined to 2 mm. This strategy resulted in a final mesh comprising approximately 1.5 million elements, with an element quality metric (such as element mass or orthogonal quality) of 0.8, which fully satisfies the established simulation requirements.

Figure 2. The turntable model after meshing

The steady-state thermal boundary conditions were defined as summarized in Table 1. The thermal power values, N_f and N_p, are subsequently applied as thermal loads in the form of heat flux to the oil seal surfaces of the radial bearing and thrust bearing, respectively. Concurrently, the appropriate material properties were assigned to the various components of the turntable. Thermal convection was incorporated at all interfaces between the turntable and the ambient, while the influence of thermal radiation was deemed negligible and therefore ignored. To ensure the accuracy and reliability of the numerical results, the automatic solution mode was selected for the solver.

Table 1. Steady-state thermal boundary conditions

Boundary conditions	**Values**
Oil inlet pressure/MPa	2
Recess pressure/MPa	1
Oil outlet pressure/MPa	0
Heat flow of Radial bearing/W	10.21
Heat flow of thrust bearing/W	19.95
Ambient temperature/℃	22

The simulated distributions of the temperature field and total deformation under varied operating conditions are illustrated in Figure 3. Analysis of the results yields the following:

Obvious thermal stratification was observed. Taking working condition (b) as an example, the highest temperature of 24.26 °C was recorded on the recess sealing surface, followed by the mandrel, while the base registered the lowest temperature at 20.47 °C. The internal temperature also follows a clear gradient, escalating along the circumferential path from the turntable's periphery towards the axis end.

Total deformation exhibits a monotonic increase from the outer edge towards the mandrel end. The turntable base displays the minimum deformation, with the maximum deformation concentrated around the motor bearing assembly. Taking mode (b) as an example, the minimum deformation of 0.62 μm occurs at the base, while the maximum deformation is observed at the motor bearing assembly, reaching 5.58 μm.

Quantitative comparison of the four working conditions shows that a 1 °C rise in temperature requires either a 13 rpm increase in speed or a 0.32 MPa increase in supply pressure. Likewise, a 1 μm increase in total bearing deformation necessitates a 10 rpm higher speed, or a 0.23 MPa higher supply pressure. It is evident that temperature rise and total deformation are positively correlated with rotational speed and supply pressure, but negatively correlated with oil film gap.

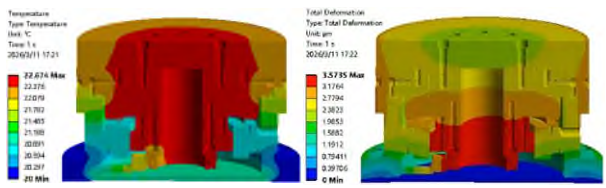

a) Mode 1(v=30rpm, h=20μm, p_s=2Mpa)

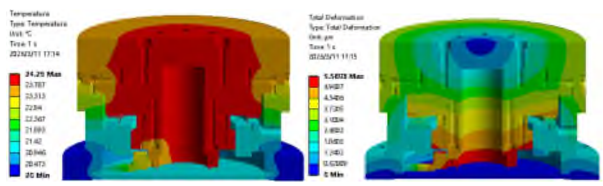

b) Mode 2(v=50rpm, h=20μm, p_s=2Mpa)

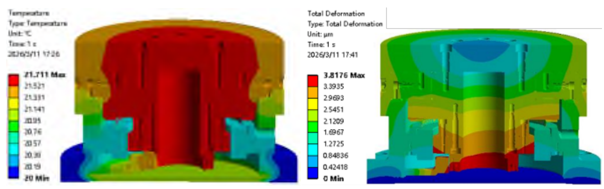

c) Mode 3(v=30rpm, h=40μm, p_s=2Mpa)

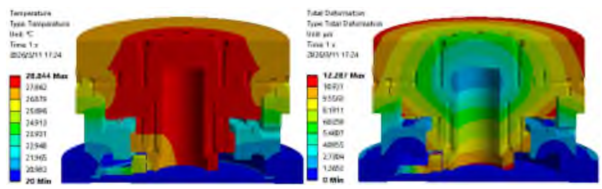

d) Mode 3(v=30rpm, h=20μm, p_s=4Mpa)

Figure 3. The temperature field and total deformation distribution of the turntable under different working conditions

4. Conclusion

To realize a quantitative improvement in the accuracy of hydrostatic turntable systems, this study successfully conducted a detailed thermal error calculation and thermo-solid coupling analysis on the system's key components. This systematic approach effectively modeled and quantified the impact of key operating parameters on the thermal error. The following main results were obtained:

A clear internal temperature stratification was identified (oil seal surface > mandrel > base) alongside a distinct axial temperature gradient.

The total deformation profile reveals a significant increase from the periphery towards the mandrel end, with the minimum deformation located at the base and the maximum at the motor bearing.

The thermal performance is influenced differently by rotational speed, oil supply pressure, and oil film gap, with oil supply pressure having a markedly stronger effect on temperature rise and total deformation than speed and oil film gap. Overall, the quantitative results presented in this paper provide a valuable new framework for the thermal error study of hydrostatic turntables, paving the way for targeted design and control strategies to enhance the system's stability and overall reliability.

Fundings

The authors gratefully acknowledge financial support from National Science and Technology Major Project (2026ZD0719001), National Natural Science Foundation of China (52575597), Genertec Group Science and Technology Innovation Project (G2025040-XA)

References

[1]Zha J, Cheng K, Xue F, Wu D X, and Liu X 2024. *Tribol*. Int. **200** 110060.
[2]Lang S, Zorzini M, Scholze S, Mayr J, and Bambach M 2025 *J. Manuf. Sys.* **80** 243-257.
[3]Wang J L, Ke C H, Hu K Y, and Zha J 2025. *Machines*, **13**(7), 598-598.
[4]Zha J, Cheng K, Wu D X, Zhang H J, and Xue F 2026. *Precis. Eng*. **97** 1060-1086.
[5]Liu T, Bei Z, Wang H, Duan R, Chen F and Zhang J 2025 *Appl. Therm. Eng.* **266** 125618-125618.
[6]Bao J, Liu X, Jiao J, Liu Z, Zhang C, Wang M, and Lin Z 2026 *Int. J. Heat. Mass. Tran.* **256** 128062-128062.